International Journal of Advanced Smart Convergence Vol.10 No.2 1-9 (2021)
http://dx.doi.org/10.7236/IJASC.2021.10.2.1

IJASC 21-2-1

Achievable Power Allocation Interval of Rate-lossless non-SIC NOMA for Asymmetric 2PAM

Kyuhyuk Chung

Professor, Department of Software Science, Dankook University, Korea
khchung@dankook.ac.kr

Abstract

In the Internet-of-Things (IoT) and artificial intelligence (AI), complete implementations are dependent largely on the speed of the fifth generation (5G) networks. However, successive interference cancellation (SIC) in non-orthogonal multiple access (NOMA) of the 5G mobile networks can be still decoding latency and receiver complexity in the conventional SIC NOMA scheme.

Thus, in order to reduce latency and complexity of inherent SIC in conventional SIC NOMA schemes, we propose a rate-lossless non-SIC NOMA scheme. First, we derive the closed-form expression for the achievable data rate of the asymmetric 2PAM non-SIC NOMA, i.e., without SIC. Second, the exact achievable power allocation interval of this rate-lossless non-SIC NOMA scheme is also derived. Then it is shown that over the derived achievable power allocation interval of user-fairness, rate-lossless non-SIC NOMA can be implemented. As a result, the asymmetric 2PAM could be a promising modulation scheme for rate-lossless non-SIC NOMA of 5G networks, under user-fairness.

Keywords: *NOMA, 5G, User-fairness, Superposition coding, Successive interference cancellation, Power allocation.*

1. Introduction

The Key feature for the convergence technologies, such as the Internet-of-Things (IoT) and artificial intelligence (AI), is fast mobile networks [1]. In such future mobile networks, non-orthogonal multiple access (NOMA) has been considered as promising technology [2-4]. High spectral efficiency and massive connectivity can be superiorities of NOMA, compared with existing orthogonal multiple access (OMA) in 4G mobile communications [5-7]. Such superiority was optimized in NOMA [8]. Cooperative NOMA was considered for full-duplex relaying [9]. Underwater visible light communication (VLC) was investigated in NOMA [10]. A power-outage tradeoff was studied for NOMA [11]. The bit-error rate (BER) performances were derived for NOMA [12], whereas local oscillator imperfection was studied for NOMA [13]. The power splitting was investigated for correlated superposition coding NOMA [14]. Also, in M-user NOMA systems, power allocation was investigated for first and second strongest channel users [15]. In addition, the achievable data rate for the asymmetric binary pulse amplitude modulation (2PAM) NOMA was derived [16]. In [16], the asymmetric 2PAM is a modulation technique which reduces inter-user interference owing to channel-sharing

Manuscript Received: March. 17, 2021 / Revised: March. 25, 2021 / Accepted: March. 28, 2021
Corresponding Author: khchung@dankook.ac.kr
Tel: +82-32-8005-3237, Fax: +82-504-203-2043
Professor, Department of Software Science, Dankook University, Korea

in NOMA. Recently, the NOMA schemes were studied for correlated information sources (CIS) [17]. In addition, negatively-CIS was investigated in [18].

Thus, in this study, in order to reduce existing latency and complexity in conventional SIC NOMA, we propose a rate-lossless non-SIC NOMA scheme for asymmetric 2PAM. First, we derive the closed-form expression for the achievable data rate of the asymmetric 2PAM non-SIC NOMA, i.e., without SIC. Second, based on numerical equivalence between asymmetric 2PAM SIC NOMA and asymmetric 2PAM non-SIC NOMA, the exact achievable power allocation interval of this rate-lossless non-SIC NOMA scheme is also derived. Then it is shown that over the derived achievable power allocation interval of user-fairness, rate-lossless non-SIC NOMA can be implemented.

The remainder of this paper is organized as follows. In Section 2, the system and channel model are described. The review of the related previous works is presented in Section 3. Achievable data rates for the non-SIC NOMA scheme with asymmetric 2PAM is derived in Section 4. In Section 5, Achievable power allocation interval of this non-SIC NOMA scheme is also derived. The results are presented and discussed in Section 6. Finally, this paper is concluded in Section 7.

The main contributions of this paper can be summarized as follows:

- We derive achievable data rates for the non-SIC NOMA scheme with asymmetric 2PAM.
- Based on such achievable data rates, we show numerically that for stronger channel user, the achievable data rate of the non-SIC NOMA scheme is almost same as that of the SIC NOMA scheme, especially with perfectly-asymmetric 2PAM.
- From such numerical equality, we derive the achievable power allocation interval of the non-SIC NOMA scheme.
- We demonstrate in numerical results that the achievable data rates of the SIC NOMA scheme can be achieved by the non-SIC NOMA scheme, over the achievable power allocation interval of user-fairness.

2. System and Channel Model

In block fading channels, the complex channel coefficient between the *m*th user and the base station is denoted by h_1 and h_2 with $|h_1| \geq |h_2|$. In this work, each receiver of all users is assumed to be equipped with a single antenna. The base station will transmit the superimposed signal $x = \sum_{m=1}^{M} \sqrt{\beta_m P_A} s_m$, where s_m is the message for the *m*th user with unit power, β_m is the power allocation coefficient (we use α_m for standard 2PAM NOMA), with $\sum_{m=1}^{M} \beta_m = 1$, $M = 2$, P is the constant total transmitted power at the base station, and P_A is the total allocated power. The observation at the *m*th user is given by

$$y_m = |h_m| x + n_m, \tag{1}$$

where $n_m \sim \mathcal{N}(0, N_0/2)$ is additive white Gaussian noise (AWGN). In this letter we assume that the standard 2PAM, $s_2 \in \{+1, -1\}$, and the asymmetric 2PAM $s_1 \in \{\pm\sqrt{2-v}, \pm\sqrt{v}\}$, are used, for the weaker and stronger channel users, respectively, where v is the asymmetric factor, $0 \leq v \leq 1$. Remark that in the

conventional NOMA, the standard 2PAM, $s_1, s_2 \in \{+1, -1\}$, are used for both users, i.e., $v = 1$. It is assumed that for the given information bits $b_1, b_2 \in \{0,1\}$, the bit-to-symbol mapping of the standard 2PAM with $v = 1$ is given by

$$\begin{cases} s_1(b_1 = 0) = +1 \\ s_1(b_1 = 1) = -1 \end{cases} \quad \begin{cases} s_2(b_2 = 0) = +1 \\ s_2(b_2 = 1) = -1 \end{cases}, \tag{2}$$

whereas the bit-to-symbol mapping of the asymmetric 2PAM with $v \neq 1$ is given by

$$\begin{cases} s_1(b_1 = 0 \mid b_2 = 0) = +\sqrt{2 - v} \\ s_1(b_1 = 1 \mid b_2 = 0) = -\sqrt{v} \end{cases}, \quad \begin{cases} s_2(b_2 = 0) = +1 \\ s_2(b_2 = 1) = -1 \end{cases},$$

$$\begin{cases} s_1(b_1 = 0 \mid b_2 = 1) = -\sqrt{2 - v} \\ s_1(b_1 = 1 \mid b_2 = 1) = +\sqrt{v}. \end{cases} \tag{3}$$

For the constant total transmitted power P at the base station, P_A is given by

$$P_A = \frac{P}{1 + 2\frac{\sqrt{1-v} - \sqrt{v}}{2}\sqrt{\alpha}\sqrt{(1-\alpha)}}. \tag{4}$$

Remark that to have the maximum interval, we only consider the asymmetric 2PAM with $v = 0$, in the rest of this paper

3. Review of Achievable Data Rate for SIC NOMA

In this section, we first present achievable data rates for asymmetric 2PAM SIC NOMA, to obtain those for asymmetric 2PAM non-SIC NOMA, although they can be found in the existing work [33]; for the first user, when perfect SIC is assumed, i.e., SIC NOMA with $r_1 = y_1 - |h_1|\sqrt{\alpha_2 P_A} s_2 = |h_1|\sqrt{\alpha_1 P_A} s_1 + n_1$, the achievable data rate $R_{1|(\mathrm{SIC})}^{(\text{asymmetric 2PAM SIC NOMA})}$ is given as

$$\begin{aligned} R_{1|(\mathrm{SIC})}^{(\text{asymmetric 2PAM SIC NOMA})} &= h(r_1 \mid b_2) - h(r_1 \mid b_1, b_2) \\ &= -\int_{-\infty}^{\infty} p_{R_1|B_2}(r_1 \mid b_2 = 0) \log_2 p_{R_1|B_2}(r_1 \mid b_2 = 0) dy_1 - \frac{1}{2}\log_2(2\pi e N_0 / 2). \end{aligned} \tag{5}$$

where

$$p_{R_1|B_2}(r_1|b_2)=\frac{1}{2}\frac{1}{\sqrt{2\pi N_0/2}}e^{-\frac{\left(r_1-|h_1|\sqrt{\alpha P_A}s_1(b_1=0|b_2)\right)^2}{2N_0/2}}+\frac{1}{2}\frac{1}{\sqrt{2\pi N_0/2}}e^{-\frac{\left(r_1-|h_1|\sqrt{\alpha P_A}s_1(b_1=1|b_2)\right)^2}{2N_0/2}}. \tag{6}$$

And for the second user, the achievable data rate $P_{2|(\text{non-SIC})}^{(\text{asymmetric 2PAM SIC NOMA})}$ is given as

$$P_{2|(\text{non-SIC})}^{(\text{asymmetric 2PAM SIC NOMA})}=\int_{-\infty}^{\infty}p_{Y_2|B_2}(y_2|b_2=0)\log_2\frac{p_{Y_2|B_2}(y_2|b_2=0)}{p_{Y_2|}(y_2)}dy_2, \tag{7}$$

where

$$p_{Y_2}(y_2)=\frac{1}{4}\frac{1}{\sqrt{2\pi N_0/2}}\left(\begin{array}{l}e^{-\frac{\left(y_2-|h_2|\sqrt{P_A}\left(\sqrt{\alpha}s_1(b_1=0|b_2=0)+\sqrt{(1-\alpha)}s_2(b_2=0)\right)\right)^2}{2N_0/2}}+e^{-\frac{\left(y_2-|h_2|\sqrt{P_A}\left(\sqrt{\alpha}s_1(b_1=1|b_2=0)+\sqrt{(1-\alpha)}s_2(b_2=0)\right)\right)^2}{2N_0/2}}\\+e^{-\frac{\left(y_2-|h_2|\sqrt{P_A}\left(\sqrt{\alpha}s_1(b_1=0|b_2=1)+\sqrt{(1-\alpha)}s_2(b_2=1)\right)\right)^2}{2N_0/2}}+e^{-\frac{\left(y_2-|h_2|\sqrt{P_A}\left(\sqrt{\alpha}s_1(b_1=1|b_2=1)+\sqrt{(1-\alpha)}s_2(b_2=1)\right)\right)^2}{2N_0/2}}\end{array}\right), \tag{8}$$

and

$$\begin{aligned}p_{Y_2|B_2}(y_2|b_2=0)=&\frac{1}{2}\frac{1}{\sqrt{2\pi N_0/2}}e^{-\frac{\left(y_2-|h_2|\sqrt{P_A}\left(\sqrt{\alpha}s_1(b_1=0|b_2=0)+\sqrt{(1-\alpha)}s_2(b_2=0)\right)\right)^2}{2N_0/2}}\\&+\frac{1}{2}\frac{1}{\sqrt{2\pi N_0/2}}e^{-\frac{\left(y_2-|h_2|\sqrt{P_A}\left(\sqrt{\alpha}s_1(b_1=1|b_2=0)+\sqrt{(1-\alpha)}s_2(b_2=0)\right)\right)^2}{2N_0/2}}.\end{aligned} \tag{9}$$

It should be noted that for $v=1$, we have

$$R_{1|(\text{SIC})}^{(\text{standard 2PAM SIC NOMA})}=R_{1|(\text{SIC})}^{(\text{asymmetric 2PAM SIC NOMA})}, \tag{10}$$

and

$$R_{2|(\text{non-SIC})}^{(\text{standard 2PAM SIC NOMA})}=P_{2|(\text{non-SIC})}^{(\text{asymmetric 2PAM SIC NOMA})}. \tag{11}$$

In addition, to clarify our contributions, we depict the rate loss owing to non-SIC, i.e., without SIC, in Fig. 1, as follows:

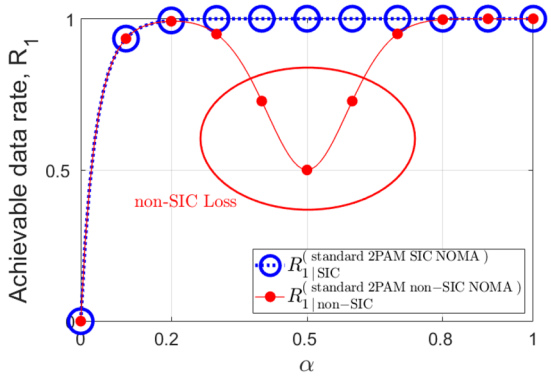

Figure 1. Illustrations for severe rate-loss of standard 2PAM SIC NOMA for first user, owing to non-SIC.

As shown in Fig. 1, the severe rate loss is observed when SIC is not perform in the standard 2PAM NOMA scheme. It should be noted that such severe rate loss is due to inter-user-interference in the non-SIC NOMA scheme. In the rest of the paper, we demonstrate rate-lossless non-SIC NOMA for asymmetric 2PAM and derive the achievable power allocation interval of this rate-lossless non-SIC NOMA.

4. Derivation of Achievable Data Rate for non-SIC NOMA

In this section, we formally derive achievable data rates for asymmetric 2PAM non-SIC NOMA; because

$$P_{2|(\text{non-SIC})}^{(\text{asymmetric 2PAM non-SIC NOMA})} = P_{2|(\text{non-SIC})}^{(\text{asymmetric 2PAM SIC NOMA})}, \tag{12}$$

we derive only $R_{1|(\text{non-SIC})}^{(\text{asymmetric 2PAM non-SIC NOMA})}$, which is given as

$$\begin{aligned} R_{1|(\text{non-SIC})}^{(\text{asymmetric 2PAM non-SIC NOMA})} &= I(y_1;b_1) \\ &= h(y_1) - h(y_1 \mid b_1). \end{aligned} \tag{13}$$

The PDF $p_{Y_1|}(y_1)$ is represented by

$$p_{Y_1|}(y_1) = \frac{1}{4}\frac{1}{\sqrt{2\pi N_0/2}}\left(e^{-\frac{\left(y_1-|h_1|\sqrt{P_A}\left(\sqrt{\alpha}c_1(b_1=0)+\sqrt{(1-\alpha)}c_2(b_2=0|b_1=0)\right)\right)^2}{2N_0/2}} + e^{-\frac{\left(y_1-|h_1|\sqrt{P_A}\left(\sqrt{\alpha}c_1(b_1=0)+\sqrt{(1-\alpha)}c_2(b_2=1|b_1=0)\right)\right)^2}{2N_0/2}} + e^{-\frac{\left(y_1-|h_1|\sqrt{P_A}\left(\sqrt{\alpha}c_1(b_1=1)+\sqrt{(1-\alpha)}c_2(b_2=0|b_1=1)\right)\right)^2}{2N_0/2}} + e^{-\frac{\left(y_1-|h_1|\sqrt{P_A}\left(\sqrt{\alpha}c_1(b_1=1)+\sqrt{(1-\alpha)}c_2(b_2=1|b_1=1)\right)\right)^2}{2N_0/2}} \right). \tag{14}$$

Then, the differential entropy is calculated by

$$\begin{aligned} h(y_1) &= -\mathbb{E}\left[\log_2 p_{Y_1|}(y_1)\right] \\ &= -\int_{-\infty}^{\infty} p_{Y_1|}(y_1)\log_2 p_{Y_1|}(y_1)\,dy_1. \end{aligned} \tag{15}$$

And the conditional differential entropy is calculated by

$$\begin{aligned} h(y_1 \mid b_1) &= -\mathbb{E}\left[\log_2 p_{Y_1|B_1}(y_1 \mid b_1)\right] \\ &= -\sum_{b_1=0}^{1} P(b_1) \int_{-\infty}^{\infty} p_{Y_1|B_1}(y_1 \mid b_1) \log_2 p_{Y_1|B_1}(y_1 \mid b_1) dy_1. \end{aligned} \tag{16}$$

where the conditional PDF is given by

$$p_{Y_1|B_1}(y_1 \mid b_1) = \frac{1}{2} \frac{1}{\sqrt{2\pi N_0/2}} \left(e^{-\frac{\left(y_1 - |h_1|\sqrt{P_A}\left(\sqrt{\alpha}c_1(b_1) + \sqrt{(1-\alpha)}c_2(b_2=0|b_1)\right)\right)^2}{2N_0/2}} + e^{-\frac{\left(y_1 - |h_1|\sqrt{P_A}\left(\sqrt{\alpha}c_1(b_1) + \sqrt{(1-\alpha)}c_2(b_2=1|b_1)\right)\right)^2}{2N_0/2}} \right). \tag{17}$$

Hence the final expression can be given as

$$R_{1|(\text{non-SIC})}^{(\text{asymmetric 2PAM non-SIC NOMA})} = -\int_{-\infty}^{\infty} p_{Y_1|}(y_1) \log_2 p_{Y_1|}(y_1) dy + \sum_{b_1=0}^{1} P(b_1) \int_{-\infty}^{\infty} p_{Y_1|B_1}(y_1 \mid b_1) \log_2 p_{Y_1|B_1}(y_1 \mid b_1) dy_1. \tag{18}$$

5. Derivation of Achievable Power Allocation Interval

To derive the achievable power allocation interval, we observe the following numerical result;

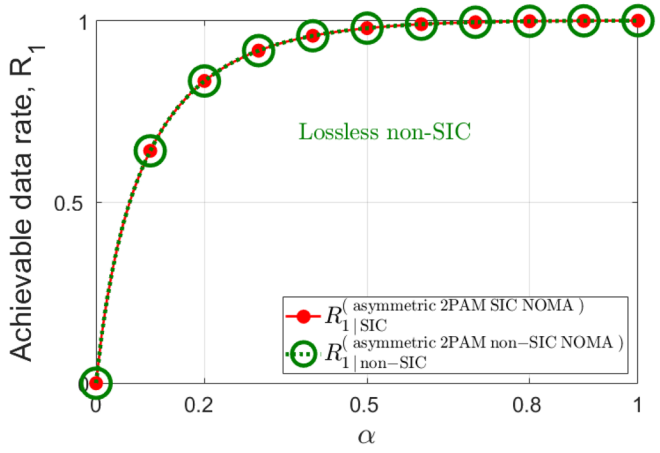

Figure 2. Comparison of achievable data rates for asymmetric 2PAM SIC/non-SIC NOMA for first user.

As shown in Fig. 2, the numerical results show that they are almost the same, although the analytical expressions for $R_{1|(\text{SIC})}^{(\text{asymmetric 2PAM SIC NOMA})}$ in and $R_{1|(\text{non-SIC})}^{(\text{asymmetric 2PAM non-SIC NOMA})}$ in are quite different. Therefore, since it is difficult to have the achievable power allocation interval from $R_{1|(\text{SIC})}^{(\text{standard 2PAM SIC NOMA})}$ and $R_{1|(\text{non-SIC})}^{(\text{asymmetric 2PAM non-SIC NOMA})}$, we obtain it from $R_{1|(\text{SIC})}^{(\text{standard 2PAM SIC NOMA})}$ and $R_{1|(\text{SIC})}^{(\text{asymmetric 2PAM SIC NOMA})}$ instead; we start our derivation from such equation

$$R_{1|(\mathrm{SIC})}^{(\text{standard 2PAM SIC NOMA})} = R_{1|(\mathrm{SIC})}^{(\text{asymmetric 2PAM SIC NOMA})}. \tag{19}$$

After some algebraic manipulations, we obtain the following closed-form equation:

$$\sqrt{\alpha} = \frac{1}{2}\left(\sqrt{\left(\frac{1}{1+2\dfrac{\sqrt{1-v}-\sqrt{v}}{2}\sqrt{\beta(1-\beta)}}\right)}\beta\sqrt{2-v} + \sqrt{\left(\frac{1}{1+2\dfrac{\sqrt{1-v}-\sqrt{v}}{2}\sqrt{\beta(1-\beta)}}\right)}\beta\sqrt{v}\right). \tag{20}$$

Notably, when $\beta = 1$, we have $\alpha = 0.5$; hence, the achievable power allocation interval is $0 \le \alpha \le 0.5$, which is calculated by, with $\beta = 1$,

$$\sqrt{\alpha} = \frac{1}{2}\left(\sqrt{\left(\frac{1}{1+0}\right)}1\sqrt{2}+0\right), \quad \sqrt{\alpha} = \frac{1}{2}\left(\sqrt{2}\right) = \frac{1}{\sqrt{2}}, \quad \therefore \alpha = \frac{1}{2} = 0.5. \tag{21}$$

6. Numerical Results and Discussions

We assumed that $|h_1| = \sqrt{1.5}$ and $|h_2| = \sqrt{0.5}$. The average total transmitted signal power to noise power ratio (SNR) is $P / N_0 = 15$. For the first user, the achievable data rates of the asymmetric 2PAM non-SIC NOMA scheme and the standard 2PAM SIC NOMA scheme are shown in Fig. 1.

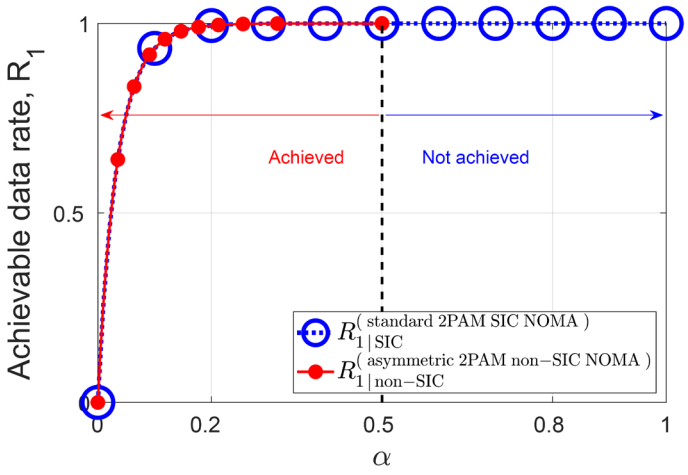

Figure 3. Achievable power allocation interval of asymmetric 2PAM non-SIC NOMA for first user.

As shown in Fig. 3, It is observed that for the first user, the achievable data rate of the asymmetric 2PAM non-SIC NOMA scheme is almost the same as that of the standard 2PAM SIC NOMA, especially without SIC. Notably, the achievable power allocation interval, i.e., $0 \le \alpha \le 0.5$, is consistent with that of user-fairness in the NOMA literature.

Then, for the second user, the achievable data rates of the asymmetric 2PAM non-SIC NOMA scheme and the standard 2PAM SIC NOMA scheme are shown in Fig. 2.

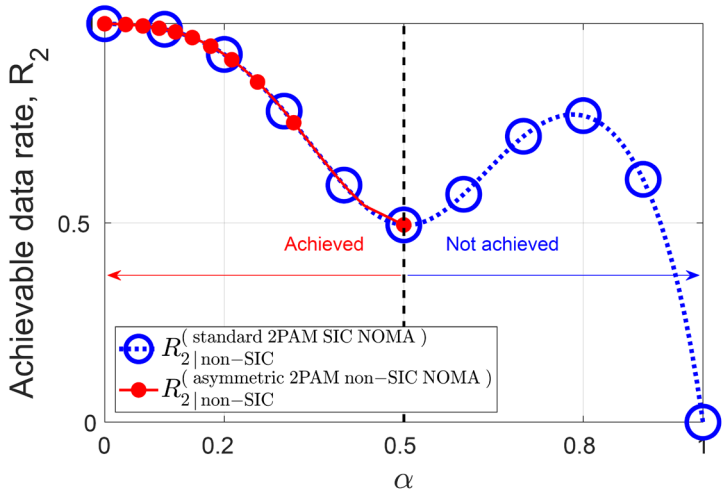

Figure 4. Achievable power allocation interval of asymmetric 2PAM non-SIC NOMA for second user.

As shown in Fig. 2, although rate-loss is not observed for the first user, the achievable data rate of the second user in the asymmetric 2PAM non-SIC NOMA scheme is also the same as that in the standard 2PAM SIC NOMA scheme. Notably, the achievable power allocation interval of $0 \le \alpha \le 0.5$ includes most of the typical values of the power allocation, so that it is sufficient to implement the practical NOMA system, under user-fairness.

7. Conclusion

In this paper, to reduce existing latency and decoding complexity in conventional SIC NOMA schemes, we proposed the non-SIC NOMA scheme for asymmetric 2PAM.

First, we derived achievable data rates for the non-SIC NOMA scheme with asymmetric 2PAM. Second, based on such achievable data rates, we showed numerically that for stronger channel user, the achievable data rate of the non-SIC NOMA scheme is almost same as that of the SIC NOMA scheme, especially with perfectly-asymmetric 2PAM. We then from such numerical equality, derived the achievable power allocation interval of the non-SIC NOMA scheme. Finally, we demonstrated in numerical results that the achievable data rates of the SIC NOMA scheme can be achieved by the non-SIC NOMA scheme, over the achievable power allocation interval of user-fairness, with asymmetric 2PAM. As a result, the existing latency and complexity of a conventional SIC NOMA scheme can reduced with the proposed non-SIC NOMA scheme, under the main NOMA principle of user-fairness.

As a direction of future researches, it would be significant to improve the BER performance of the weaker channel gain user with the proposed modulation scheme and non-SIC decoding.

References

[1] L. Chettri and R. Bera, "A comprehensive survey on internet of things (IoT) toward 5G wireless systems," *IEEE Internet of Things Journal*, vol. 7, no. 1, pp. 16–32, Jan. 2020. DOI: https://doi.org/10.1109/JIOT.2019.2948888

[2] Y. Saito, Y. Kishiyama, A. Benjebbour, T. Nakamura, A. Li, and K. Higuchi, "Non-orthogonal multiple access (NOMA) for cellular future radio access," in *Proc. IEEE 77th Vehicular Technology Conference (VTC Spring)*, pp.

1–5, 2013. DOI: https://doi.org/10.1109/VTCSpring.2013.6692652

[3] Z. Ding, P. Fan, and H. V. Poor, "Impact of user pairing on 5G nonorthogonal multiple-access downlink transmissions," *IEEE Trans. Veh. Technol.*, vol. 65, no. 8, pp. 6010–6023, Aug. 2016. DOI: https://doi.org/10.1109/TVT.2015.2480766

[4] Z. Ding, X. Lei, G. K. Karagiannidis, R. Schober, J. Yuan, and V. Bhargava, "A survey on non-orthogonal multiple access for 5G networks: Research challenges and future trends," *IEEE J. Sel. Areas Commun.*, vol. 35, no. 10, pp. 2181–2195, Oct. 2017. DOI: https://doi.org/10.1109/JSAC.2017.2725519

[5] S. Kim, "Link adaptation for full duplex systems," *International Journal of Advanced Smart Convergence (IJASC)*, vol. 7, no. 4, pp. 92-100, Dec. 2018. DOI: http://dx.doi.org/10.7236/IJASC.2018.7.4.92

[6] S. Kim, "Switching between spatial modulation and quadrature spatial modulation," *International Journal of Advanced Smart Convergence (IJASC)*, vol. 8, no. 3, pp. 61–68, Sep. 2019. DOI: http://dx.doi.org/10.7236/IJASC.2019.8.3.61

[7] S. Kim, "Transmit antenna selection for quadrature spatial modulation systems with power allocation," *International Journal of Advanced Smart Convergence (IJASC)*, vol. 9, no. 1, pp. 98–108, Mar. 2020. DOI: http://dx.doi.org/10.7236/IJASC.2020.9.1.98

[8] Z. Chen, Z. Ding, X. Dai, and R. Zhang, "An optimization perspective of the superiority of NOMA compared to conventional OMA," *IEEE Trans. Signal Process.*, vol. 65, no. 19, pp. 5191–5202, Oct. 2017. DOI: https://doi.org/10.1109/TSP.2017.2725223

[9] Z. Yong, V. W. S. Wong, and R. Schober, "Stable throughput regions of opportunistic NOMA and cooperative NOMA with full-duplex relaying," *IEEE Trans. Wireless Commun.*, vol. 17, no. 8, pp. 5059–5075, Aug. 2018. DOI: https://doi.org/10.1109/TWC.2018.2837014

[10] M. Jain, N. Sharma, A. Gupta, D. Rawal, and P. Garg, "Performance analysis of NOMA assisted underwater visible light communication system," *IEEE Wireless Commun. Lett*., vol. 9, no. 8, pp. 1291-1294, Aug. 2020. DOI: https://doi.org/10.1109/LWC.2020.2988887

[11] Z. Sun, Y. Jing, and X. Yu, "NOMA design with power-outage tradeoff for two-user systems," *IEEE Wireless Commun. Lett.*, vol. 9, no. 8, pp. 1278-1282, Aug. 2020. DOI: https://doi.org/10.1109/LWC.2020.2987992

[12] M. Aldababsa, C. Göztepe, G. K. Kurt, and O. Kucur, "Bit Error Rate for NOMA Network," *IEEE Commun. Lett*., vol. 24, no. 6, pp. 1188-1191, Jun. 2020. DOI: https://doi.org/10.1109/LCOMM.2020.2981024

[13] A.-A.-A. Boulogeorg, N. D. Chatzidiamantis, and G. K. Karagiannid, "Non-orthogonal multiple access in the presence of phase noise," *IEEE Commun. Lett*., vol. 24, no. 5, pp. 1133-1137, May. 2020. DOI: https://doi.org/10.1109/LCOMM.2020.2978845

[14] K. Chung, "On power splitting under user-fairness for correlated superposition coding NOMA in 5G system," *International Journal of Advanced Smart Convergence (IJASC)*, vol. 9, no. 2, pp. 68-75, Jun. 2020. DOI: http://dx.doi.org/10.7236/IJASC.2020.9.2.68

[15] K. Chung, "On power calculation for first and second strong channel users in *M*-user NOMA system," *International Journal of Advanced Smart Convergence (IJASC)*, vol. 9, no. 3, pp. 49-58, Sept. 2020. DOI: http://dx.doi.org/10.7236/IJASC.2020.9.3.49

[16] K. Chung, "Analysis on achievable data rate of asymmetric 2PAM for NOMA," *International Journal of Advanced Smart Convergence (IJASC)*, vol. 9, no. 4, pp. 34-41, Dec. 2020. DOI: http://dx.doi.org/10.7236/IJASC.2020.9.4.34

[17] K. Chung, "NOMA for correlated information sources in 5G Systems," *IEEE Commun. Lett*., vol. 25, no. 2, pp. 422-426, Feb. 2021. DOI: https://doi.org/10.1109/LCOMM.2020.3027726

[18] K. Chung, "Achievable sum rate of NOMA with negatively-correlated Information Sources," *International Journal of Advanced Smart Convergence (IJASC)*, vol. 10, no. 1, pp. 75-81, Mar. 2021. DOI: http://dx.doi.org/10.7236/IJASC.2021.3.1.75